FORM TI-12
2/99

B-T-3262

MEAN STRESS AND ENVIRONMENTAL EFFECTS ON FATIGUE IN TYPE 304 STAINLESS STEEL

G. L. Wire, T. R. Leax, J. T. Kandra
April 1999

DE-AC11-98PN38206

BETTIS ATOMIC POWER LABORATORY WEST MIFFLIN, PENNSYLVANIA 15122-0079

Operated for the U.S. Department of Energy
by Bechtel Bettis, Inc.

DISCLAIMER

DISCLAIMER

Portions of this document may be illegible in electronic image products. Images are produced from the best available original document.

MEAN STRESS AND ENVIRONMENTAL EFFECTS ON FATIGUE IN TYPE 304 STAINLESS STEEL

G. L. Wire, T. R. Leax, and J. T. Kandra
Bechtel Bettis, Inc
West Mifflin, Pennsylvania 15122-0079

ABSTRACT

Fatigue life tests were performed in air on Type 304 stainless steel (304 SS) to establish the effect of mean stress under both load control and strain control. An apparent reduction of up to 26% in strain-amplitude occurred in the low and intermediate cycle regime ($<10^6$ cycles) for a mean stress of 138 Mpa. A quantitative description of mean stress effects using the Smith-Watson-Topper equivalent strain parameter was developed, which incorporates mean stress through the maximum stress. This description provided a tighter fit to the data, and allowed separation of mean stress and cold work effects. With this separation, the effect of mean stress was reduced to 12% decrease in strain amplitude at 138 Mpa. The stress-life curve apparently increased with increasing mean stress, due to the significant work hardening that occurred in tests with high mean stresses, especially under load control.

Tests were performed on double-edge notched specimens of 304 SS in air and low oxygen water at 288°C. The elastically calculated increase in the notch tip stress accounted within 10% for the fatigue life reductions for a K_t =4.8 notch, but was 38% conservative for a K_t = 8.8 notch. Fatigue crack initiation lives (defined as an 0.127 mm crack) in low oxygen water at 288°C were reduced by a factor of four to eight on cycles over those in air. Crack growth occurred throughout most of the fatigue "initiation" life. The increase in crack growth rate of 304 SS in water appears to be large enough to explain the reduced "initiation" life in this environment.

I. INTRODUCTION

Over the past several years, there has been considerable discussion of the large degradation in the fatigue life of austenitic stainless steels in high temperature water and the incorporation of this effect into a design equation (Chopra and Smith, 1998). Effects of mean stress can also degrade the fatigue life of these steels. The ASME fatigue design curve does not include a mean stress correction below 10^6 cycles since the fatigue strength at 10^6 cycles is higher than the monotonic yield strength. There is little data in the literature to verify the applicability of this approach in the life regime below 10^6 cycles. A series of tests on cylindrical specimens were performed to assess mean stress effects in air. The test results were analyzed both qualitatively and by use of the Smith-Watson-Topper equivalent strain parameter, which provides a convenient formulation for design analysis based on the strain-life behavior.

A separate series of tests were performed on notched uniaxial specimens in both water and air to assess the effects of notch radius and environment on fatigue "initiation" life, defined at a crack extension of 0.127 mm. Use of the electrical potential difference (EPD) technique allowed detection of small cracks and their growth rate without removal from the autoclave. Results were compared to the smooth fatigue data on the same heat of material using the elastically calculated notch stress.

II. MEAN STRESS EFFECTS

A. EXPERIMENTAL

Conventional tensile fatigue life tests were performed in air on Type 304 stainless steel for the primary purpose of establishing the effect of mean stress. Other parameters varied in this study were temperature, the heat of material, and the type of test control (i.e., load versus strain control).

The materials used in this study were two heats of Type 304 stainless steel. The vendor chemical compositions and mechanical properties of these heats are given in Tables 1 and 2, respectively. Both heats were procured as cylindrical forgings, with a diameter of 127 mm for the Heat 42322, which was used for almost all of the tests. Testing revealed much wider variations in mechanical properties than indicated by the vendor properties. Room temperature yield stresses varied

from 259-352 MPa at different locations in the forging, and as a result, fatigue properties also varied significantly with specimen location. At 288°C, yield strength varied from 152-338 MPa. These wide variations are attributed to variations in working from the surface to the center of the thick cylindrical forgings.

A cylindrical tensile/fatigue specimen was used in the tests. The gauge length was 19.1 mm with a diameter of 5.1 mm. In all cases, the tensile axis of the specimen was parallel to the longitudinal direction of the forgings. Fatigue tests were performed to ASTM 606 with failure defined as the complete separation of the specimen into two halves. Test results are provided in Tables 3 and 4.

Samples were fatigue tested in strain control with applied strain amplitudes ranging from 0.11% to 0.70% at both room temperature and 288°C. The tests utilized either 0% mean strain or 1% mean strain with the first half cycle of the test in compression. In addition, four specimens were tested at significantly higher mean strains to compare to tests under load control with high strains. The frequency was 0.5 Hz unless the test exceeded 200,000 cycles. At 200,000 cycles, the test was switched to load control at the current stress level and the frequency increased to five Hz, in order to complete the tests more quickly. Maximum and minimum stresses were recorded at cycle one and periodically throughout the test. Some test specimens were precycled 20 cycles at room temperature to ± 1% strain in an attempt to produce higher mean stresses via cyclic hardening.

Load control enabled mean stress tests to be performed at controlled, constant mean stresses and to increase the level of mean stress. In contrast, the mean stress frequently decreased to near zero by half-life in the strain-controlled tests, especially at high strain amplitudes. The test parameters for the load control tests were largely modeled after the strain-controlled tests at cycle one with the goal of maintaining a high, positive mean stress for the duration of the test.

B. DESCRIPTION OF TEST RESULTS

The results of the strain and load controlled tests are given in Tables 3 and 4, respectively. The stresses are engineering stresses, with the values at half life used for the strain controlled tests. The strain-controlled tests demonstrate an effect of mean stress over the data range, as shown in Figure 1. All of the data points with high mean stress (σ_m >34 MPa) lie below the trend curve for the entire data set. In order to overcome data scatter and obtain a qualitative estimate of mean stress effects, it was desirable to utilize all the data simultaneously to establish a baseline curve. The effects of mean stress were fit as a reduction in the strain amplitude $-\varepsilon_a(1-\alpha\sigma_m)$ –patterned after the Goodman model. The least squares fit result gives a reduction due to mean stress of α=0.0023/MPa, with 95 percent limits of ±0.0013/MPa. This best fit line is shown in Figure 1, along with a reduced line for a mean stress of 138 MPa. The uncertainty on the calculated mean stress effects is large when all of the data are weighted equally, and is due mostly to large scatter from the tests at low mean stress. To overcome this effect, a fit was made using a weighting factor proportional to the mean stress. The result is α=0.0019/MPa showing much reduced 95% confidence limits of ±0.0002/MPa. The estimated effects of mean stress are a 26% relative reduction in strain amplitude at a mean stress of 138 MPa. However, this estimate depends sensitively on the zero mean stress reference curve. The analysis in Section C below using the Smith-Watson-Topper parameter (Smith, Watson, and Topper, 1970) overcomes this difficulty, and is preferred for quantitative purposes.

The load controlled tests provided nine additional fatigue tests with mean stress values over 117 MPa. Strain amplitudes were measured only during the first five cycles, so the strain amplitude at half-life might well be different. However, for strain amplitudes, ε_{amp} <0.15%, it was considered appropriate to compare these test results directly to the strain controlled data. This more than doubled the amount of high mean stress data available. As shown in Figure 2, the strain amplitudes from load controlled test results with mean stresses to 245 MPa are easily bounded by the line at 138 Mpa mean stress developed from the strain controlled tests.

These results are very similar to those for steels and aluminum (Fuchs and Stevens, 1980). The data on the steels and especially on the aluminum alloys show the wide scatter typical of the stainless steel results. For the maximum ratio of mean stress to ultimate tensile stress of $\sigma_m/\sigma_u \approx 0.3$, the average reductions in stress amplitude were 20-40% for steels and aluminum alloys, similar to the present stainless steel test results. It is therefore concluded that the effects of mean stress on fatigue life are similar among these different alloys and that the effect is modest below $\sigma_m/\sigma_u = 0.5$.

C. QUANTITATIVE MODEL OF MEAN STRESS EFFECTS ON THE STRAIN-LIFE CURVE

The traditional methods usually employed for accounting for mean stress effects (Goodman, 1899), (Gerber, 1874)), or (Morrow, 1968) cannot be used to describe mean stress effects on 304 stainless steel since these models rely on changes in the stress-life curve due to imposed mean stresses to quantify the effect of mean stress. Basing a mean stress effect model solely on the load controlled tests would result in an apparent increase in the fatigue strength with increasing mean stress due to the large uniaxial strains and corresponding extensive cold work which occurs when imposing a large mean stress in load control (see discussion below). Consequently, the model chosen for characterizing mean stress effects on 304 stainless steel is one first described in a more simplified form by Smith, Watson, and Topper (1970). The form of the model is as follows:

$$\mathrm{LOG}(N_f) = A + B \bullet \mathrm{LOG}(\varepsilon_{eq} - \varepsilon_o) \qquad (1)$$

where: ε_{eq} is an equivalent strain given by:

$$\varepsilon_{eq} = \varepsilon_a^c \bullet \left(\frac{\sigma_{max}}{E}\right)^{1-c}$$

ε_a is the total strain amplitude (mm/mm)
σ_{max} is $\sigma_a + \sigma_{mean}$
E is Young's modulus
A, B, c, and ε_0 are fitting parameters.

Some of the strain-controlled tests were conducted at a mean strain of 1% to 10%, as shown in Table 3, so the calculated stresses based on the original cross-sectional area underestimate the true stresses in the test specimens. Consequently, the nominal mean stress and stress amplitude in Tables 3 and 4 were corrected for straining by assuming the test specimens maintain a constant volume when plastically deformed:

$$\sigma_{corrected} = \sigma_{nominal} \bullet (1 + \varepsilon_r) \qquad (2)$$

where: $\sigma_{nominal}$ is the measured load at half-life divided by the original cross-sectional area
ε_r is the permanent strain in the test specimen at the end of the test (mm/mm)
$\sigma_{corrected}$ is the stress at the end of the test.

A least squares fit of the data to Equation 1 gave the following values for the fitted parameters:

A = -4.31 - 0.2*PS
B = -3.35
c = 0.831
ε_0 = 0.

As shown in Figure 3, the difference between zero mean strain and positive mean strain data is significant. Hence, this difference is due to both mean stress and prestraining. PS is a dummy variable equal to zero for those zero mean strain tests where the test specimen was not given 20 cycles at ∓1% strain prior to testing. PS is equal to 1 for tests where the mean strain was ≥1% or for zero mean strain tests where the test specimens were precycled at ∓1% strain prior to the start of testing. The need for this term in the model is unexpected and indicates that prestraining, either monotonically or cyclically, has a small detrimental effect (factor of 1.6 on cycles) on fatigue life. This could be due to the effects of the higher mean stresses present at the beginning of the test which relax by half-life, to a reduction in the surface compressive residual stresses (induced by specimen machining) due to these large initial strains, or to some other unidentified cause.

A plot of the observed versus fitted values from this curve fit is shown in Figure 4, showing a much tighter fit to the data, as can by seen by comparison to Figure 1. A plot of fatigue life as a function of the Smith-Watson-Topper equivalent strain is shown in Figure 5. In this latter plot, the data from the zero mean strain tests are shown as solid circles and the data from tests where the mean strain was ≥1% are shown as open circles. Where appropriate, the data have been corrected for the effect of prestraining. Separate least squares fits to the two data sets are shown in the plot and clearly demonstrate that the Smith-Watson-Topper model is able to accurately account for the effects of mean stress on the strain-life curve.

The value of c in Equation (1) is an indicator of the relative effect of mean stress on fatigue behavior. A value near zero indicates a large effect of mean stress, while a value of unity indicates no effect. The relatively large value of c for 304 stainless steel indicates that mean stress has a relatively small effect on fatigue life. This model predicts a reduction of approximately 12% in the fatigue strength (on a strain amplitude basis) at 10^6 cycles for an applied mean stress of 138 MPa. Accounting for the effects of strain history reduced the sensitivity to mean stress, compared to the data analysis in Section B. With this model, the zero mean stress strain-life curve is always above the predicted curve for a finite mean stress. It is worth noting that if the effects of pre-strain are added to the effects of mean stress, the total reduction is 27%, the same as obtained in the analysis in Section B.

Very few data are available in the literature on the effect of mean stress on the fatigue behavior of austenitic stainless steels between room temperature and 288°C. These data are not sufficient to define mean stress effects conclusively at intermediate strain amplitudes. Data from Soo and Chow (1977) shows that, in the high cycle regime, imposition of a mean stress of 45 MPa decreases the fatigue strength by approximately 5% at room temperature for $N \geq 3x10^5$. Results reported by Manjoine and Tome (1983) indicate that imposition of a mean stress equal to the alternating stress only decreases the fatigue strength of 347 stainless steel by 6% at 10^8 cycles and 316°C. The magnitude of the mean stress effect from these studies is therefore consistent with the model developed above for mean stress effects on the strain-life curve.

D. EFFECT OF MEAN STRESS ON THE STRESS-LIFE CURVE

A stress-life plot obtained from load-controlled tests is shown in Figure 6. Tests performed with low mean stresses (<68.9 MPa) are plotted as circles while tests with high mean stresses (≥68.9 MPa) are shown as squares. All of the stress values are corrected for plastic straining which generally occurred on the first cycle at levels up to 14% strain. Surprisingly, the specimens subjected to high mean stresses appear to have somewhat higher fatigue strength. To confirm this observation, the data (excluding runouts) were fit to the following equation using nonlinear least squares:

$$\mathrm{LOG}(N_f) = A + B \bullet \mathrm{LOG}\left(\frac{\sigma_{a,corrected}}{1 - \frac{\sigma_{m,corrected}}{S'}}\right) \qquad (3)$$

where: N_f is the number of cycles to failure
$\sigma_{a,corrected}$ is the corrected stress amplitude
$\sigma_{m,corrected}$ is the corrected mean stress

A, B, S' are fitting constants

For this data set:

A = 11.6
B = -5.24
S' = -369 MPa

This model provides a good fit to the data; a plot of the observed versus fitted values is shown in Figure 7. The negative value for S' indicates that an increase in the mean stress correlates to an increase in the fatigue strength. As noted previously, this is likely due to the work hardening from the large initial strains that occurred in tests with positive mean stresses. The results of strain controlled tests at room temperature and 288°C with both zero and positive mean strains were also fit to this model. The value of S' determined from this set of data is –377 MPa, almost identical to the value of S' determined from the mean stress tests in load control. These results indicate that increasing mean stress correlates to an increase in fatigue strength (on a stress basis) due to the cold work required to maintain a mean stress in 304 SS.

Similar results to the ones presented here have been reported for cold worked and annealed 304 stainless steel (Rao, et al.,1993) and for 304LN stainless steel given different amounts of cold work (Raman and Padmanabhan, 1996). These investigations show that when comparing cold worked and annealed material, or when comparing material given increasing amounts of cold work, the stress-life curve for the lower strength condition is below the stress-life curve for the higher strength condition. Ten to fifteen percent plastic strains occurred in the load controlled tests with high mean stresses (>138 MPa) on initial loading, leading to increases in the true yield stress of up to 207 MPa. Hence, work hardening was significant and it would be expected that the fatigue strength on a stress-life basis would be improved. The plastic strain-life curves, however, are expected to display the opposite behavior.

III. ENVIRONMENTAL EFFECTS ON NOTCHED SPECIMENS

A. EXPERIMENTAL

304 SS specimens were machined from a 127 mm diameter forging of heat Number 42322 procured to MIL-S23195D. This heat of 304 SS material is the same as used in most of the tests defining mean stress effects, described above. The material was tested in the as-received condition. The chemical composition of this material is provided in Table 1 and mechanical properties are provided in Table 2.

A double-edge notched uniaxial specimen was utilized in these tests. The specimen dimensions were as follows: width=38.1 mm, thickness=5.1 mm, and notch depth of 4.8 mm. Two notch root radii were tested-0.38 mm (K_t = 8.8) and 1.52 mm (K_t = 4.8). This specimen has an advantage over compact tension specimens in that it can be tested in both tensile and compressive loading conditions. Additionally, the notch defines the point of crack initiation, facilitating the use of the Electric Potential Difference (EPD) measurement for the detection of crack initiation and crack growth.

The tests were performed under load control in an autoclave, including most of the tests in an air environment. Five of the tests in air were performed in a more conventional fatigue fixture, facilitating frequent optical measurements for calibration. Alignment was achieved by manually adjusting the pull rod while monitoring strain gages attached to the specimen. Once a satisfactory alignment was achieved, the strain gages were removed and the EPD leads were attached. The assembly was then enclosed in an autoclave, which was filled with water and heated to 288°C. The specimen was cycled until crack initiation was detected, based on an EPD reading corresponding to a crack depth of 0.127 mm. This value was chosen to represent the minimum crack extension detectable with assurance, and minimize the contribution of crack growth. Following an interim visual inspection, cycling was continued until the longest crack reached 1.27 mm by EPD indication.

Flowing deaerated water containing 20-60 ml H_2/kg water was employed in the water tests. Dissolved oxygen was therefore generally less than 10 ppb. The room temperature pH was in the range 10.1 to 10.3. The pH at 288°C was estimated[1] to be 6.5 to 6.7.

B. TEST RESULTS

1. Environmental Effects

As previously reported (Chopra and Smith, 1998; Higuchi and Iida, 1997) 304 SS exhibits significant environmental effects. As shown in Figure 8a and 8b, the effects of environment can be estimated directly by comparing results in air and water for each notch root radius. The effects of environment are approximately a reduction in cycles by factors of four at the larger notch radius, shown in Figure 8a. The effects seem to be larger at the smaller notch radius, about a factor of eight. While it is clear that the data are very limited, these reduction factors appear to be in the minimum appropriate given the present limited database. Literature data in low oxygen water shows environmental effects on 304 SS and 316 SS as large or larger than observed herein ((Chopra and Smith,1998), up to a factor of 15 at low strain rates.

2. Mean Stress Effects

The tests were almost all fully reversed, with $R=\sigma_{max}/\sigma_{min}=-1$. The two specimens tested with R = 0 (positive mean stress) showed reduced life compared to those at R = -1 (zero mean stress) in both air and water, as shown in Figure 8a. With the rather large scatter effects noted above on smooth specimens, it appears that these observed reductions on single specimens must be considered to be only qualitative. It is noted that the percentage reduction in stress for a given fatigue life is of order 15% from the trend curve for 304 SS in air

[1] Calculated using MULTEQ[R] Electric Power Research Institute

and slightly less in deaerated water, as may be seen in Figure 8a. This reduction is qualitatively consistent with results from the large number of tests performed on smooth specimens.

3. Notch Effects

The effect of the differing notch root radius on 304 SS fatigue life can be seen qualitatively in Figure 8 both in air and water. For example, at a nominal stress of about 75 MPa, data are available for both notch radii and environments. At this stress level, the cycles to failure for the larger notch root radius are larger by about a factor of five in water and about a factor of three in air. The factor of five on cycles is roughly equivalent to a factor of 1.6 on stress, a strong effect. However, the analysis is qualitative because the test frequency in water is lower for the more sharply notched specimen, which may have contributed to part of the notch effect.

The reduction of allowed stress at a given fatigue life due to the stress concentrations can be quantitatively compared to the elastically calculated stress concentration factors for the tests performed in air. The elastic stress concentrations, calculated using finite element analysis, were: K_{tg} (gross stress) = 4.8 for the 1.52 mm notch radius and K_{tg} = 8.8 for the 0.38 mm notch radius. The elastically calculated strain amplitude for a given test is then calculated as $K_{tg}*\sigma_g/E$. These values were compared to finite element calculations (Wilson, 1974) and were typically within 10 % for the test series.

The elastically calculated values overestimated the effect of notches for K_t=8.8. Consequently, the fatigue notch factor K_f was calculated to describe the notch effects. The calculated magnitude of K_f was that value providing the best fit of the notched data with the smooth specimen results. Using the nominal fits to the smooth specimen data in Figure 1, the K_f values of 4.3 and 5.5 were derived from experiment for the two notch radii. The experimental notch factor is very close to the theoretical value at the larger notch radius. Notch effects at the smaller radii are considerably over predicted by the theoretical 8.8 factor, with the actual factor being about 5.5. This large overestimate of notch effects at smaller notch radius is apparently not due to a plasticity effect, as the strain calculated by finite element analysis (Wilson, 1974) for notched compact tensions changed by only about 3% (relative) over the K_t range of 4-8. Another possible explanation is that the elastically calculated concentration factors may fail to correlate well because a significant portion of the fatigue initiation life actually involves crack growth, as discussed below.

4. Crack Growth

EPD data from these tests were analyzed to determine crack depths for the notched tests described above. Cracks at 0.127 mm depth, the value defined here for fatigue initiation, are typically referred to as mechanically short cracks, and their growth rates may be different from those determined from tests on conventional compact tension specimens. The plot in Figure 9 is a simple moving average of the raw data. The Figure shows that crack growth is occurring very soon after the start of cycling in air. In fact, a crack growth rate of 9.4×10^{-7} mm/cycle was assessed at 8500 cycles, while the initiation criteria of 0.127 mm crack depth was met at 32500 cycles. Crack growth therefore accounted for at least 75% of the fatigue life under these test conditions in air.

The effect of environment on crack growth rates can be assessed by comparing the test results in air and water under identical loading conditions. By comparing tests at R=0, the potential effects of crack closure are minimized. Further, the stress amplitudes are identical, eliminating the need for adjustments to the data. The relative rates in air and water are shown in Figure 10 for a crack depth of 0.05 mm. The crack growth rates are about a factor of eight higher in water than in air even at small crack extensions, for this condition with R=0, 0.033 Hz in water. The reduction in fatigue initiation life in deaerated water compared to air was typically about 4 to 8 for 304 SS, as shown in Figure 8, and was about 4 for the R=0 tests. Hence, the increase in crack growth rate in water is large enough to account for the environmental degradation in water. Such a large increase in crack growth rates in water would be significant by itself for applications where short cracks are of concern.

IV. SUMMARY AND CONCLUSIONS

Fatigue life tests were performed in air on Type 304 stainless steel (304 SS) to establish the effect of mean stress under both load control and strain control. An apparent reduction of up to 26% in strain-amplitude occurred in the low and intermediate cycle regime ($<10^6$ cycles) for a mean stress of 138 Mpa. A quantitative description of mean stress effects using the Smith-Watson-Topper equivalent strain parameter was developed, which incorporates mean stress through the maximum stress. This description provided a tighter fit to the data, and allowed separation of mean stress and cold work effects. With this separation, the effect of mean stress was reduced to 12% decrease in strain amplitude at 138 Mpa.

These results are consistent with mean stress effects observed in steels and aluminum alloys, which show about a 20% degradation due to mean stress at the corresponding ratio of mean stress to ultimate stress. For 304 SS, the stress-life curves actually increased with increasing mean stress due to the significant work hardening which occurred in tests with high mean stresses, especially under load control. This observed increase in stress-life is consistent with the fact that cold-worked stainless steels have higher fatigue strengths than annealed material.

The effect of notch radius on fatigue life is comparable to elastically calculated stress concentration factors at K_t=4.8, but significantly less at K_t=8.8. Potential difference data were analyzed to determine the crack growth rates for mechanically short cracks emanating from notches. These data show that most of the "initiation" life, defined as the number of cycles needed to produce a crack depth of 0.127 mm, is

actually spent in the growth of mechanically short cracks. For tests at R=0 at 0.033Hz, the crack growth rates increased by a factor of about eight in water, while the fatigue initiation life was reduced by about four. Hence, the observed increase in crack growth rates of short cracks in water can account for the reduction in fatigue life.

ACKNOWLEDGEMENTS

The authors would like to acknowledge the key contributions of H. K. Shen and A. J. Bradfield for initiation of these tests, W. J. Mills for suggesting the potential difference technique for fatigue testing, to R.S.Piehler for the stress concentration analysis, and especially to the many people in the Corrosion Laboratory and Mechanical Test Laboratory for their exacting performance of the tests.

REFERENCES

1) Chopra, O. K. and Gavenda, D.J., 1997, "Effects of LWR Coolant Environments on Fatigue Lives of Austenitic Stainless Steels", PVP Vol. 353, Pressure Vessel and Piping Codes and Standards, ASME, pp. 87-97

2) Chopra, O. K. and. Smith,J. L ,1998, "Estimation of Fatigue Strain-Life Curves for Austenitic Stainless Steels in Light-Water Reactor Environments", PVP Vol. 374, Pressure Vessel and Piping Codes and Standards, ASME, pp. 249-259

3) Fuchs, H. O. and. Stephens, R. I, 1980, Metal Fatigue in Engineering, Wiley, pp 69-76

4) Gerber, W. J, 1874, bayer. Archit. Ing. Ver., Vol. 6, p. 101

5) Goodman, J., 1899, Mechanics Applied to Engineering, Longman, Green & Co., London

6) Higuchi, M. and Iida, K., 1997, "Reduction in Low-Cycle Fatigue Life of Austenitic Stainless Steels in High-Temperature Water", PVP-Vol. 353, Pressure Vessel and Piping Codes and Standards, ASME, pp. 79-85

7) Manjoine, M. J. and Tome, R. E., 1983, "Proposed Design Criteria for High Cycle Fatigue of Austenitic Stainless Steel", International Conference on Advances in Life Prediction Methods, D. A. Woodford and J. R. Whitehead, eds, ASME, pp.51-57

8) Morrow, J., 1968, "Fatigue Properties of Metals", Section 3.2 of Fatigue Design Handbook, SAE

9) Raman, S. G. S. and Padmanabhan, K. A., 1996, "Effect of Prior Cold Work on the Room-Temperature Low-Cycle Fatigue Behavior of 304LN Stainless Steel", Int. J. Fatigue, Vol. 18, No. 2, pp. 71-79

10) Rao, K. B. S., Valsan, M., Sandhya, R., Mannan, S. L. and Rodriguez, P., 1993, "An Assessment of Cold Work effects on Strain-Controlled Low-Cycle Fatigue Behavior of type 304 Stainless Steel", Met. Trans. A, Vol. 24A, pp. 913-924

11) Smith, K. N., Watson, P. and. Topper, T. H, 1970, "A Stress-Strain Function for the Fatigue of Metals", J. Materials, ASTM, Vol. 5, No. 4, pp. 767-778

12) Soo, P. and Chow, J. G. Y., 1977, "The Effects of Mean Tensile Stresses on High-Cycle Fatigue Life and Strain Accumulation in Some Reactor Materials", BNL-NUREG-50654, Brookhaven National Laboratory

13) Wilson, W.K, 1974, "Elastic-Plastic Analysis of Blunt Notched CT Specimens and Applications", J. Pressure Vessel Technology, Trans. ASME, Vol. 96, No. 4, p. 293

TABLE 1. Materials Chemistries

Element	C	Mn	P	S	Si	Cr	Ni	Mo
42322	0.04	1.49	0.026	0.001	0.36	18.43	8.85	0.29
1L793	0.018	1.81	0.035	0.006	0.37	18.14	8.84	0.32
Element	Cu	Co	N	Fe	Al	Ti	B	Mg
42322	0.18	0.08	0.039	Bal				
1L793	--	--	--	Bal.	--	--	--	--

TABLE 2. Vendor Mechanical Properties

Heat	42322		1L793	
Run	1	2	1	2
Hardness (BHN)	143	140	--	--
Yield Stress (MPa)	288	266	269	273
Ultimate Tensile Stress (MPA)	545	550	572	572
Elongation (%)	67.2	68.0	72	71
Reduction of Area (%)	80.4	80.8	81.9	82

TABLE 3. Strain Controlled Test Results

Temperature (°C)	Precycle (Y/N)	ε_a (mm/mm)	ε_{mean} (%)	N_f	σ_a (Mpa) at half-life	σ_m (Mpa) at half-life
22	N	0.007	0	1235	367	0.7
22	N	0.007	0	1110	374	-3.4
22	N	0.0045	0	3694	287	-3.4
22	N	0.0046	0	5016	263	1.4
22	N	0.0026	0	2000000+	250	-6.9
22	N	0.0026	0	76481	236	1.4
22	N	0.0023	0	2000000+	226	-0.7
22	N	0.0023	0	2000000+	196	-6.2
22	N	0.0032	0	42795	279	-1.4
22	N	0.0028	0	77923	261	2.1
22	N	0.0032	1	9201	241	19.3
22	N	0.0032	1	6438	261	15.9
22	N	0.0028	1	11748	276	35.2
22	N	0.0028	1	15529	237	20.7
22	N	0.0023	1	48657	234	33.1
22	N	0.0023	1	22984	260	32.4
22	N	0.002	1	45403	222	21.4
22	N	0.0018	1	27338	279	130
22	N	0.004	2	2927	291	11.0
22	N	0.016	1	67114	219	41.4
22	N	0.0024	0	29960	237	-2.8
22	N	0.0013	1	219050	203	82.7
22	N	0.00109	1	2000000+	185	98.6
288	N	0.0045	0	8345	221	-6.2
288	N	0.0045	0	8475	216	-9.0
288	N	0.0024	0	20351	191	-1.4
288	N	0.0024	0	32189	163	-6.9
288	N	0.002	0	92033	154	-5.5
288	N	0.0018	0	82677	209	-11.7
288	N	0.0016	0	131795	206	17.2
288	N	0.0026	1	20934	168	-4.8
288	N	0.0024	1	37215	187	4.8
288	N	0.002	1	22083	229	24.8
288	N	0.002	1	30019	203	18.6
288	N	0.0016	1	89163	151	4.1
288	N	0.0014	1	158677	202	91.0
288	N	0.00109	1	7000000+	145	34.4
288	Y	0.00168	0	171393	244	-1.4
288	Y	0.001995	0	24381	208	0

TABLE 3. Strain Controlled Test Results (Cont'd.)

Temperature (°C)	Precycle (Y/N)	ε_a (mm/mm)	ε_{mean} (%)	N_f	σ_a (Mpa) at half-life	σ_m (Mpa) at half-life
288	Y	0.00231	0	31412	194	-1.4
288	Y	0.0017	1	29948	198	27.7
288	Y	0.00198	1	32418	238	44.1
288	Y	0.0023	1	31723	206	15.2
288	Y	0.00298	0	20990	190	7.6
288	Y	0.00123	1	209078	175	83.4
288	Y	0.00299	1	21751	229	9.0
288	Y	0.0035	1	18002	184	-0.7
288	Y	0.00448	1	8753	197	0.7
288*	N	0.00739	0	3342	245	-0.7
288*	N	0.00349	0	17910	182	2.1
288*	N	0.00229	0	46383	170	-4.8
288*	N	0.00169	0	134816	167	-5.5
288*	N	0.00619	6	2200	257	-2.1
288*	N	0.00269	9	23447	213	-11.7
288*	N	0.00149	10	95312	193	142
288*	N	0.001375	10	112914	187	153

*Denotes Heat 1L793 + Runout

Table 4 Load Controlled Test Results (288°C)

N_f	ε_r (mm/mm)	σ_a (MPa)	σ_m (MPa)	ε_a – 5th cycle (mm/mm)
2000000+	0.007	100	107	0.0006
2000000+	0.013	141	38	0.0008
10727	0.007	186	0	0.0019
9773	0.027	194	2.4	0.002
15393	0.001	190	-3.4	0.0017
37531	0.002	176	3.4	0.0018
2000000+	0.012	131	82.7	0.0012
2000000+	0.044	155	93.1	0.0012
28924	0.047	179	41.3	0.0016
6004	0.008	210	-3.4	0.0033
12763	0.066	193	13.8	0.0020
6894	0.093	210	10.3	0.0027
828	-0.025	269*	0	0.0083
2826	0.14	248*	0	0.0052
7737	-0.056	214*	-13.8	0.0018
237741	0.076	155	203	0.0012
231084	0.1	153	205	0.0013
237259	0.102	152	206	0.0012
182019	0.136	169	190	0.0014
208288	0.083	162	162	0.0013
401105	0.099	158	201	0.0012
2000000+	0.118	138	221	0.0006
2000000+	0.155	124	234	0.001
2000000+	0.144	121	238	0.001
2000000+	0.123	114	245	0.0009
392064	0.14	134	224	0.0012
3695	-0.087	224*	-17.2	0.0034
131847	0.096	169*	196	0.0015

*Denotes Heat 1L793 + Runout

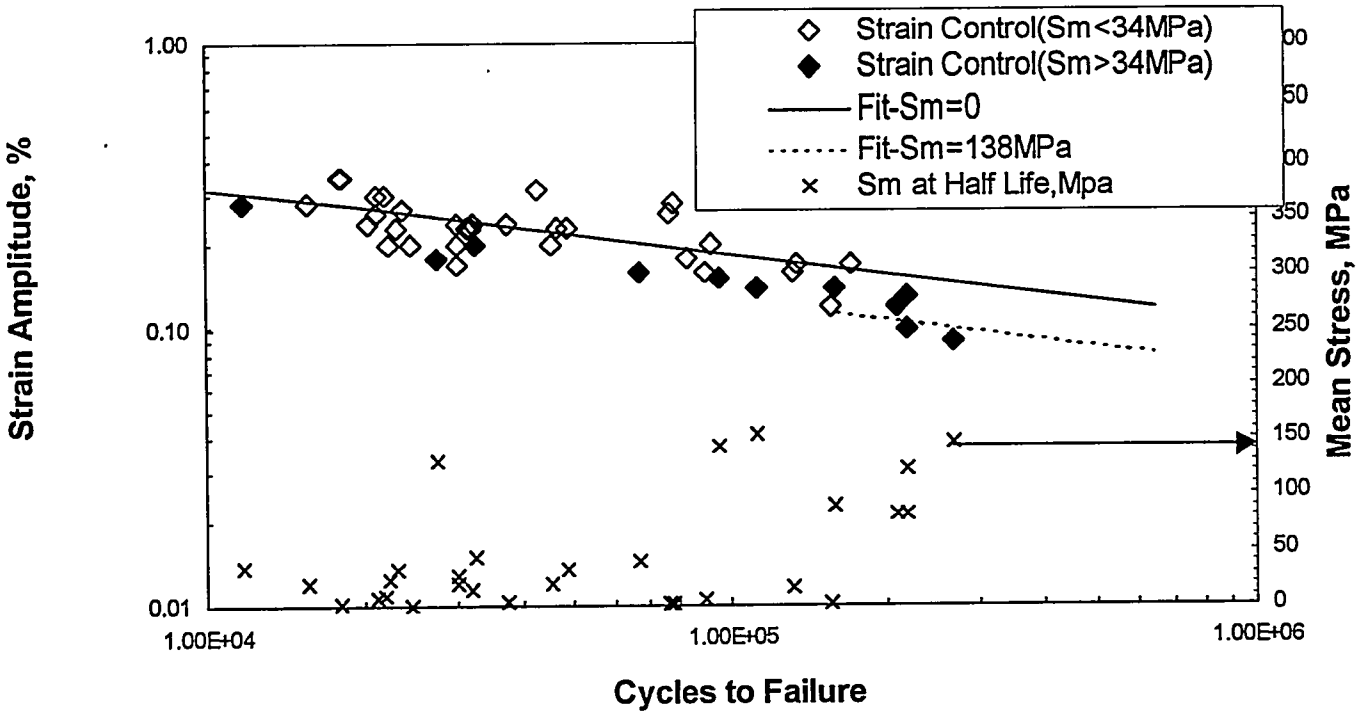

Figure 1. Mean Stress Effects in Strain Control

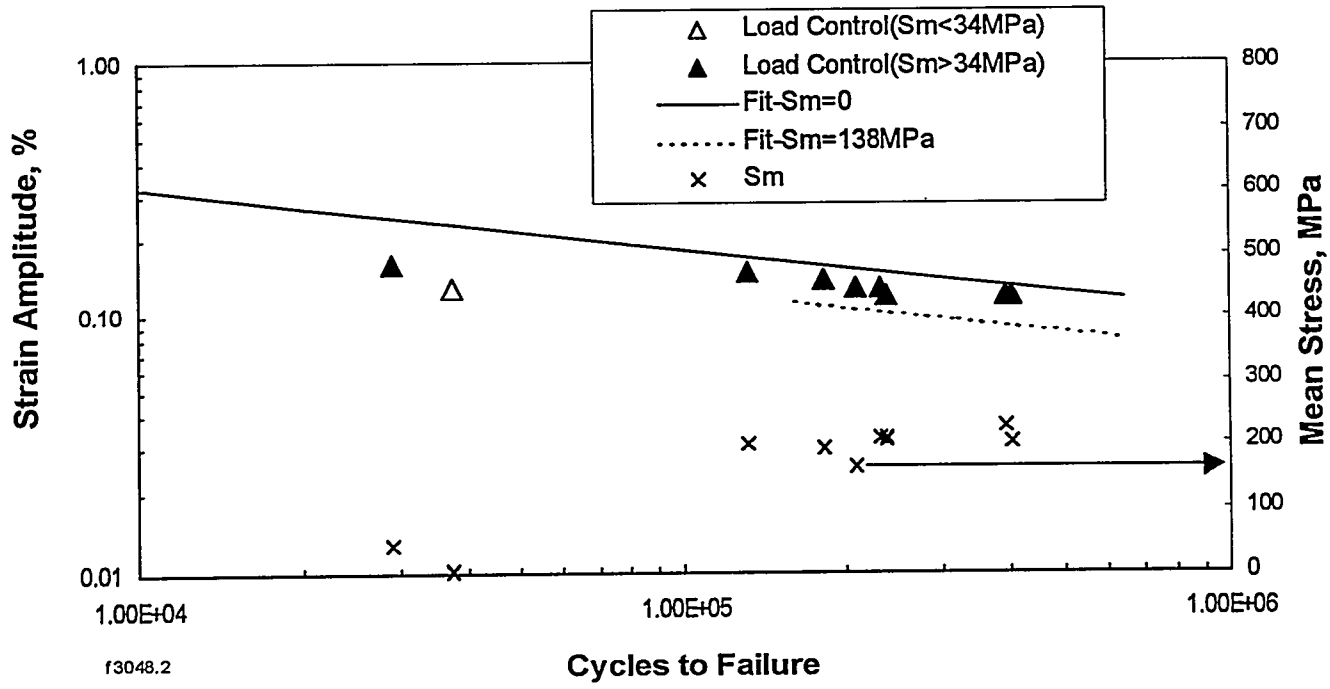

Figure 2. Mean Stress Effects in Load Control
Note Load Control Bounded by Mean Strain Results

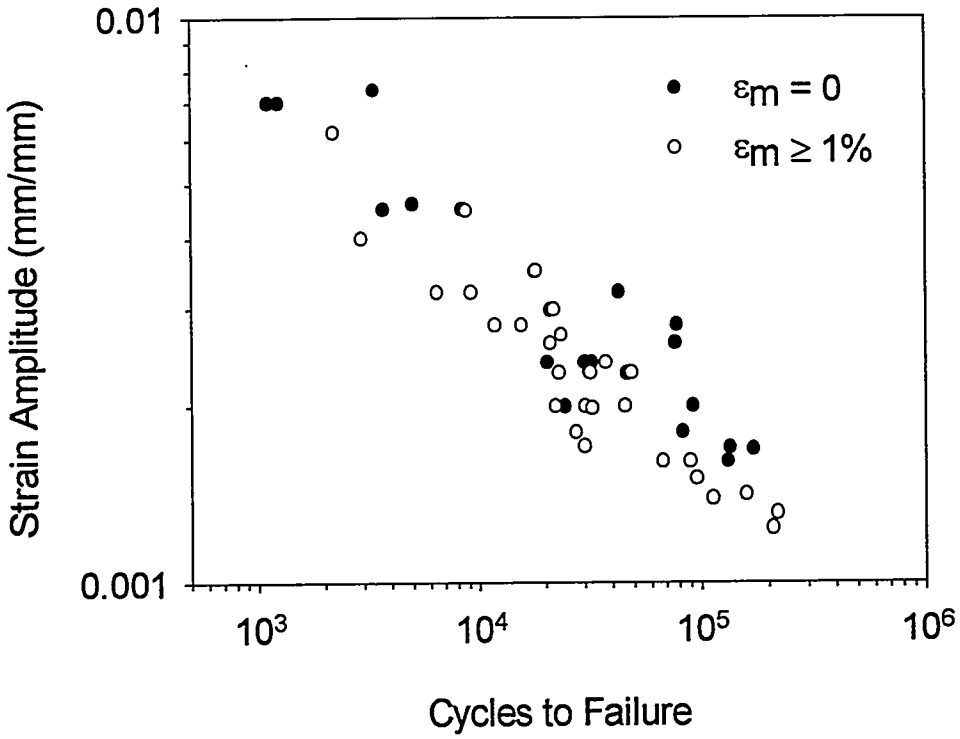

Figure 3. Effects of Prior Strain History On Fatigue Life

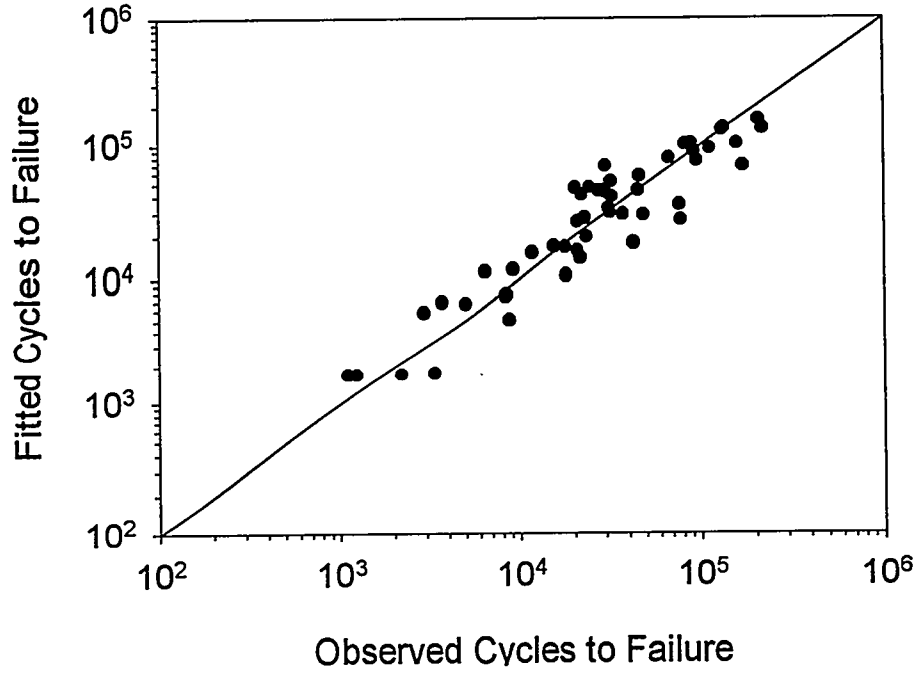

Figure 4. Experimental Versus Fitted Fatigue Lives Using Smith-Watson-Topper Parameter

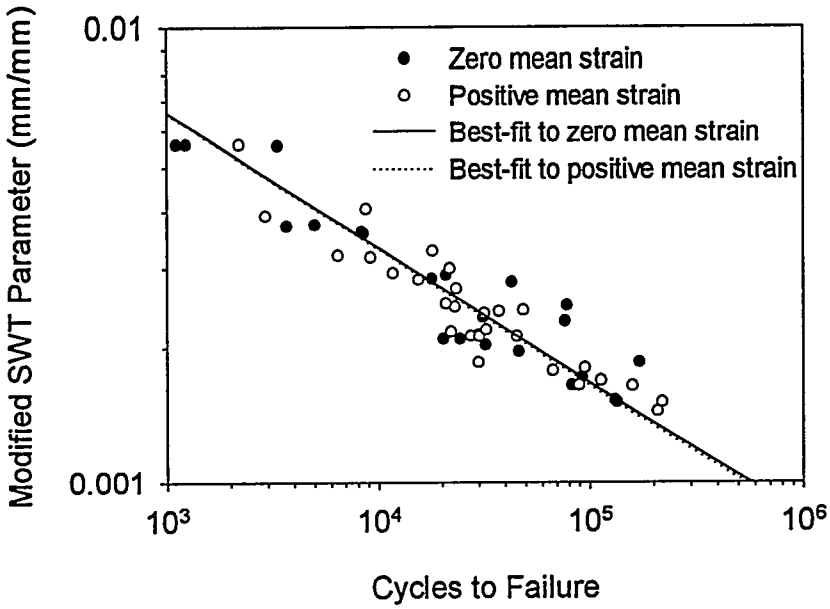

Figure 5. Fatigue Life as a Function of Smith-Watson-Topper Equivalent Parameter

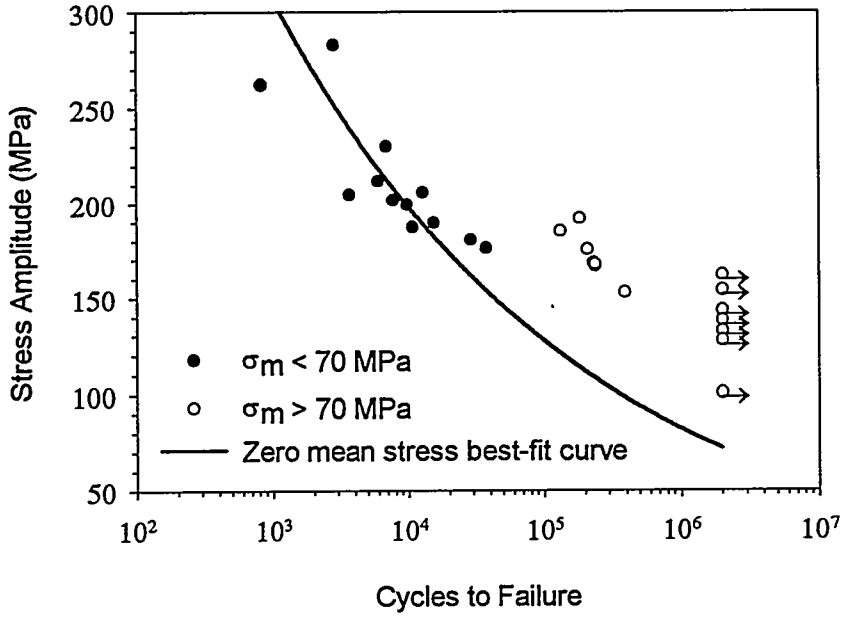

Figure 6. Stress-Life Data from the Load Controlled Fatigue Tests

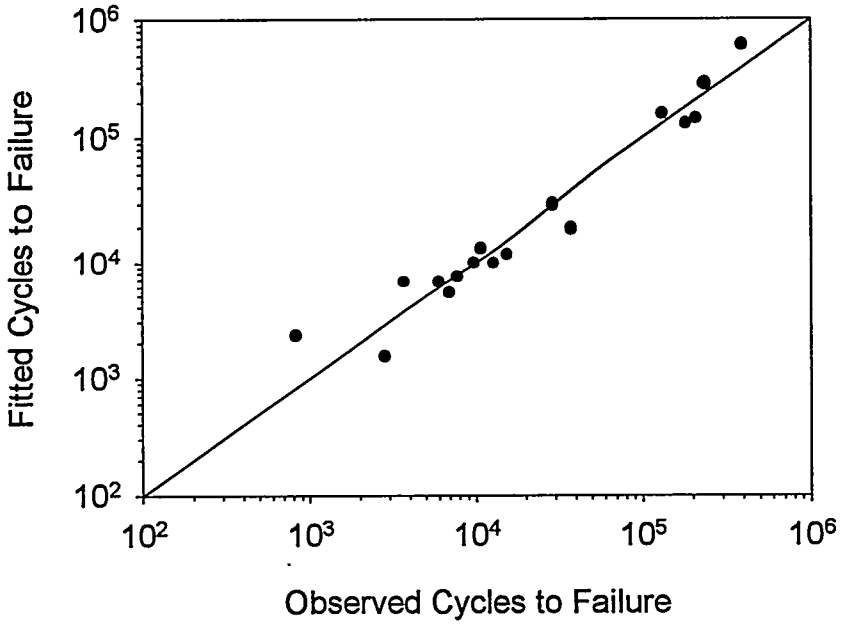

Figure 7. Experimental Versus Fitted Fatigue Lives from the Load Controlled Tests

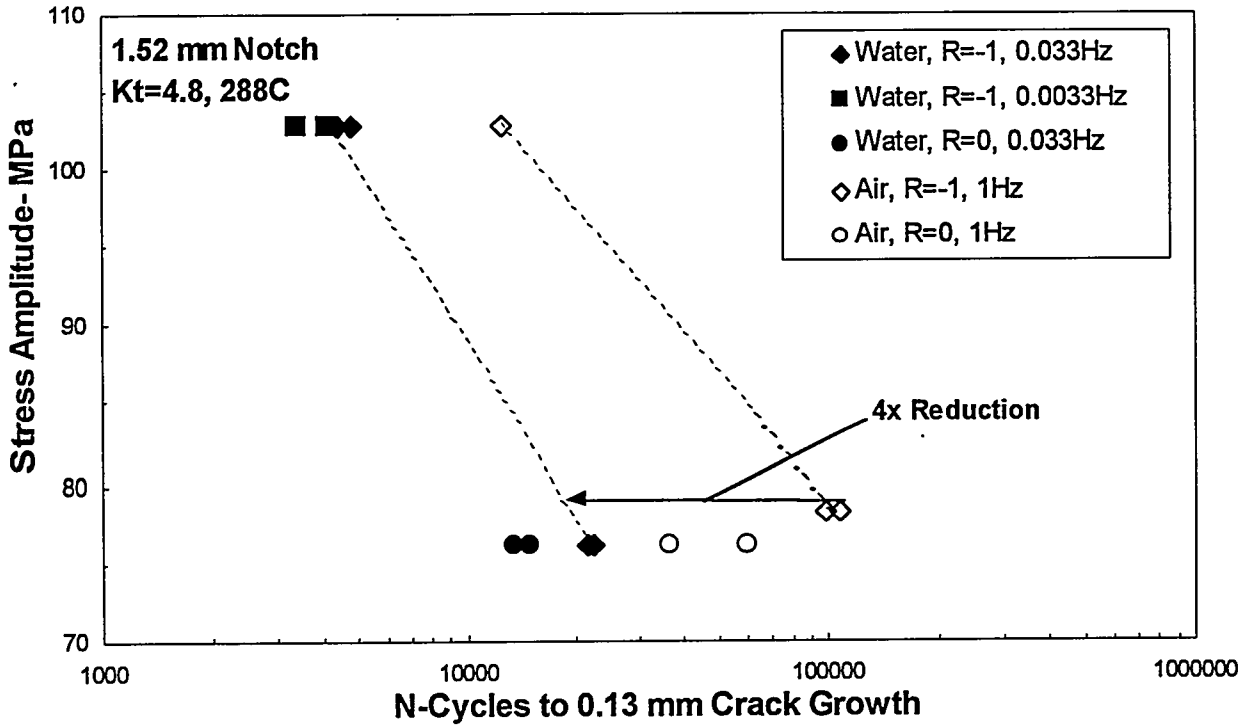

Figure 8a. Effects of Environment on Fatigue (1.52 mm notch)

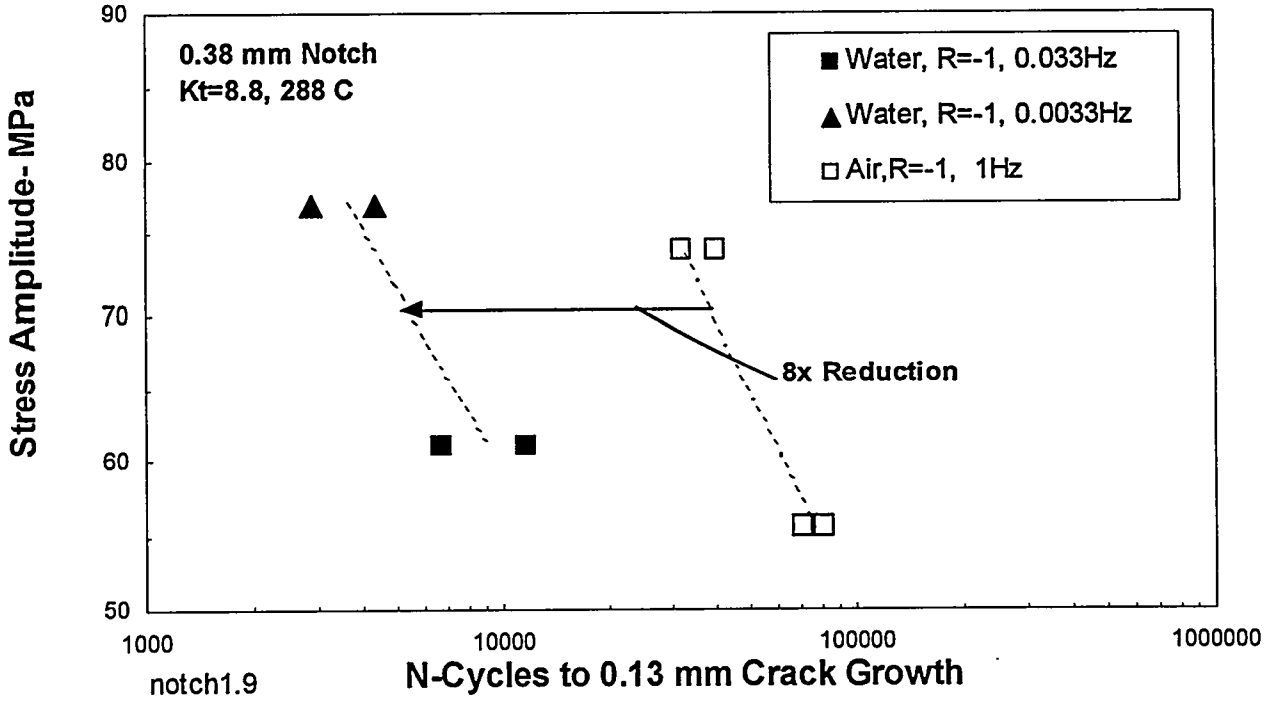

Figure 8b. Effects of Environment on Fatigue (0.38 mm notch)

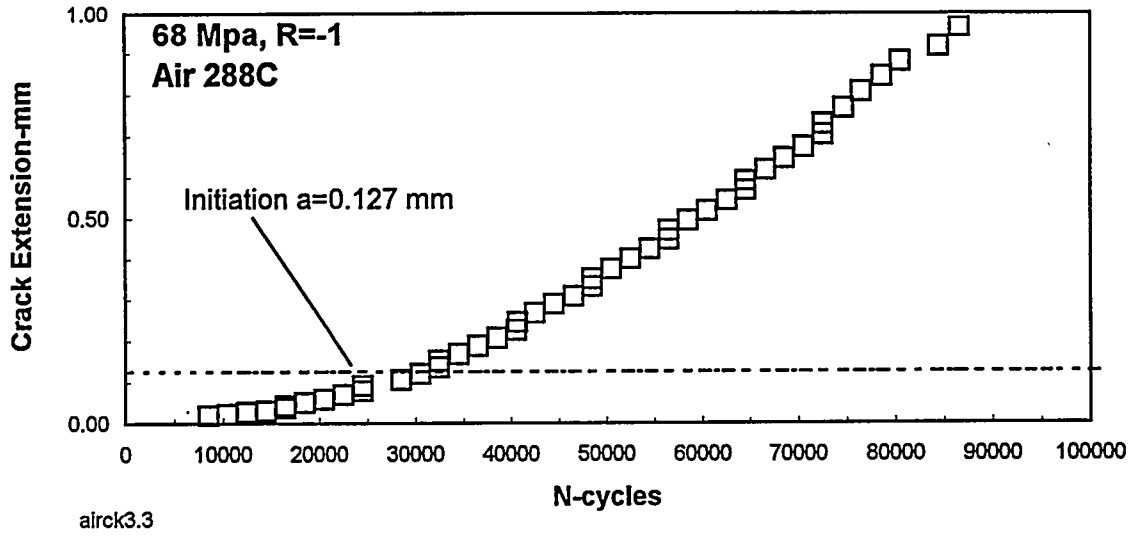

Figure 9. Crack Growth Occurs Early in "Fatigue Initiation" Life

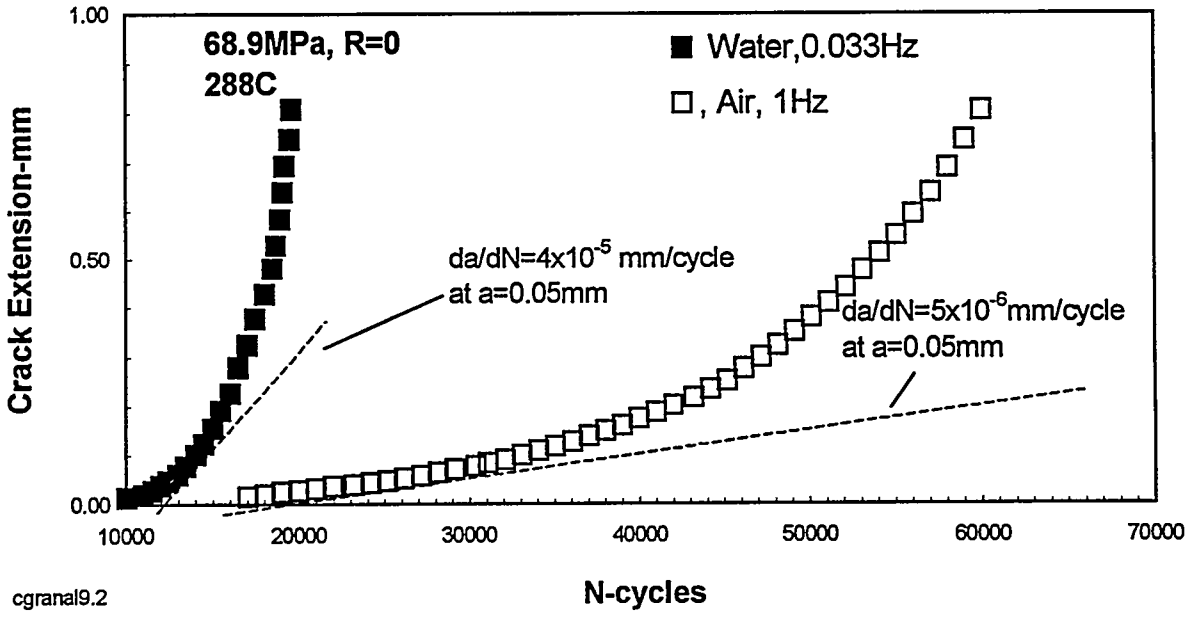

Figure 10. Crack Growth Rates 8X Higher in Water (a=0.05 mm)